Exsolution-enhanced reverse water-gas shift chemical looping activity of Sr2FeMo0.6Ni0.4O6- double perovskite

Feasibility study of a passive pneumatic exoskeleton for upper limbs based on a McKibben artificial muscle

Stefania Magnetti Gisolo[1], Giovanni Gerardo Muscolo[2], Maria Paterna[1], Carlo De Benedictis[1,*], Carlo Ferraresi[1]

[1] Department of Mechanical and Aerospace Engineering, Politecnico di Torino, Turin, Italy
[2] Department of Computer Science, University of Verona, Verona, Italy
carlo.debenedictis@polito.it

Abstract. Exoskeletons are wearable structures or systems designed to enhance human movement and to improve the wearer's strength or agility, providing auxiliary support aimed at reducing efforts on muscles and joints of the human body. The aim of this work is to discuss on the feasibility of a new passive upper limb exoskeleton, based on the use of pneumatic artificial muscles, and characterized by extreme lightness, cheapness, and ease of use. A broad overview of the state of the art on current exoskeletons is introduced. Then the concept of the new device is presented, and different transmission architectures between pneumatic muscle and limb are discussed. The study demonstrates the potential effectiveness of such a device for supporting an operator in heavy work condition.

Keywords: passive exoskeleton, pneumatic artificial muscles, deformable actuators, wearable systems, mechanisms.

1 Introduction

The exoskeleton technology originally focused on military and rehabilitation applications. In the last years, attention is paid to the application of these systems into manufacturing industry. The exoskeletons can be actuated actively or passively [1], depending on the kind of support to be provided. Active exoskeletons require an external power source in order to supply and control the actuation system, which could be pneumatic, hydraulic or electric. Due to their power consumption and battery life, they have reduced load capacity and poor power-to-weight ratio. On the other hand, passive exoskeletons cannot actively assist or control human motion but they use mechanical elements (like springs or dampers), which can store and release energy when required by the human body, without significantly increasing the inertia of the whole system. Even though passive exoskeletons are potentially less effective, they are lighter and simpler because no control is present, providing a high power-to-weight ratio.

Most of the devices available in the literature and on the market use electric motors or pneumatic muscles as actuators, and the actuation unit is usually external, or located on the user's back. To reduce the size and inertia of such systems, cable-based

actuation is often used as an alternative to separate electric DC motor for each revolute joint. Cable-driven exoskeletons can also be designed to implement speed reductions with low friction forces and zero backlash [2−4]. The main advantage of these systems is their capability of allowing a natural motion of the shoulder complex by adding passives Degrees of Freedom (DoF). In other solutions [5, 6], pulleys are used to transmit the motion to the actuation system, although a high number of idle pulleys can be often required to widen the workspace, increasing the bulkiness of the device and the occurrence of friction related issues. Complex architectures as 7 DoF upper limb exoskeletons require particular attention to avoid singularities that can occur in some configurations. Moreover, misalignments between the human arm joint axes and the exoskeleton joint axes can lead to discomfort and pain and should be taken into account during design [7−10].

Thanks to their intrinsic deformability and similarity to human muscles, pneumatic artificial muscles (PAMs) [2] have been employed in systems interacting with human beings, providing safety, compliant behavior, and higher power-to-weight ratio than electric motors [11]. The main drawbacks of this technology are the reduced stroke, the high nonlinear behavior which requires sophisticated control, and the unidirectional tension force. Mainly to improve the stroke of these deformable actuators, as well as to overcome the limitations in terms of the direction of the force exerted, several architectures have been developed for the transmission of the motion between the PAM and the end effector [12−14]. Given their passive characteristics when inflated with pressurized air, PAMs can also be employed as passive elements within the structure of an exoskeleton to provide a support for the user, similarly to spring-based systems that use elastic components to balance the effects of gravity, reducing weight and volume with respect to active solutions [15, 16].

For industrial applications, the aim is typically to assist workers in load handling, repetitive movements, overhead manipulation of objects and relieving them from excessive physical fatigue in manual tasks, always guaranteeing the user's movements and providing a relatively high shoulder flexion angle. Due to their advantages, passive devices are mostly employed. In particular, they often include passive spring-based mechanisms and leverages to provide the assistive torque at the shoulder [17−21].

The aim of this work is to present a novel passive upper limb exoskeleton meant to assist the user keeping his arms in elevated position, based on a McKibben PAM, with a lightweight structure and simple architecture. The design of the device is presented and its feasibility is discussed by means of simulations, in particular regarding the different solutions adopted to convey the tension force generated by the PAM to the end effector placed on the arm of the user.

2 Materials and Methods

2.1 Original design of the exoskeleton and PAM modeling

During overhead handling tasks, the torque created by the weight of the arms should be balanced by the contraction of the human shoulder complex muscles. If the user is

required to keep the arm lifted for a long time, a compensating device can be necessary to reduce the human shoulder effort, and to hold that position. The torque due to gravity to be compensated can be calculated from the inertial body parameters [22], and it assumes a maximum value when the elevation angle θ_1 of the upper arm (mainly in flexion) with respect to vertical position is 90° and the forearm elevation angle θ_2 is 0° (see Fig. 1).

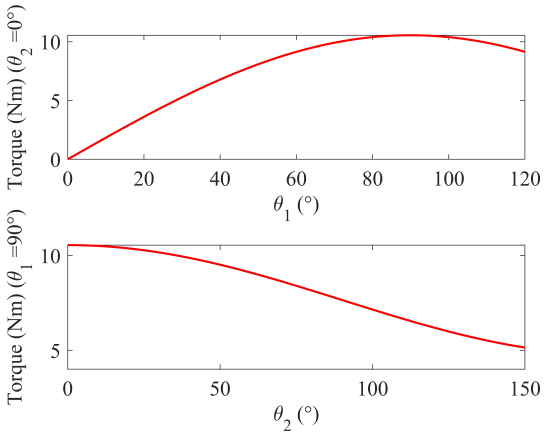

Fig. 1. Torque due to gravity with respect to the elevation angle of the upper arm θ_1 and the forearm flexion angle θ_2.

To verify the feasibility of the use of McKibben muscles in the exoskeleton, it was decided to consider the heaviest working condition, and to study the behavior of the system when only the elevation angle θ_1 varies, while maintaining the angle θ_2 of flexion of the forearm equal to zero.

The torque shown in Fig. 1 (at the top), plus an eventual contribution due to external loads exerted on the arm of the operator, should be partially or totally provided by the exoskeleton, depending on the application and on the physical characteristics of the user. The forearm was considered extended to simulate a typically laborious position, however similar considerations can be deduced for other configurations.

A simple representation of the device studied in this work is presented in Fig. 2. In the original design (Fig. 2, left), a transmission based on cable and pulley is used to transmit the PAM tension force to the bracelet (i.e., the end effector) located on the user's upper arm. Alternatively, the fixed pulley could be replaced by a fixed passing point for the cable. With respect to the scheme shown in Fig. 2 (left), the geometric parameters a, c_0, α and β are constant, so the segment c can be calculated:

$$c = c_0 / \cos\beta \tag{1}$$

By neglecting the fixed pulley radius, b is the distance of the attachment point of the cable on the arm's support with respect to the pulley, and it is only function of the elevation angle θ_1. The angle γ is calculated as:

$$\gamma = \cos^{-1}\left(\frac{b^2 + c^2 - a^2}{2bc}\right), \quad b = \sqrt{a^2 + c^2 + 2ac\cos(\theta_1 + \beta - \alpha)} \tag{2}$$

By calculating the semi-perimeter S and the area A of the triangle (a, b, c), the lever arm r of the tension force produced by the pneumatic muscle is:

$$r = 2A/b, \quad A = \sqrt{S(S-a)(S-b)(S-c)}, \quad S = (a+b+c)/2 \tag{3}$$

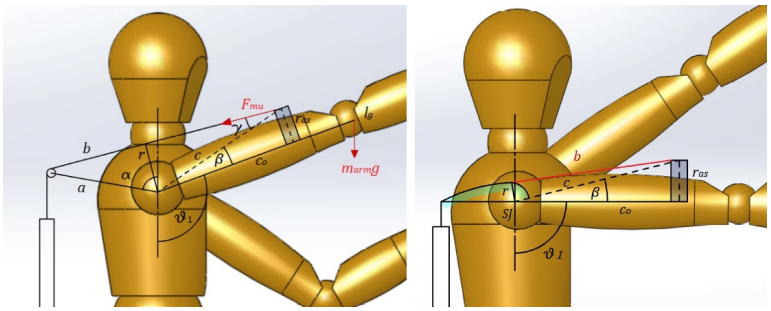

Fig. 2. Different designs of the exoskeleton: original design (left), cam-based design (right).

Among the several solutions available, a commercial McKibben artificial muscle (DMSP-20-200N, Festo, Germany, nominal length l_0=0.21 m) has been considered for this application. A static characteristics of the force exerted by the pneumatic muscle, function of the percentage contraction k and of the relative supply pressure p, has been produced, using the exponential function to approximate the modified Hill's muscle model, through MATLAB Curve Fitting Toolbox (The MathWorks, USA) [23], see Fig. 3:

$$F_{mu} = (a_1 p + a_2)e^{a_3 k} + a_4 kp + a_5 p + a_6 \tag{4}$$

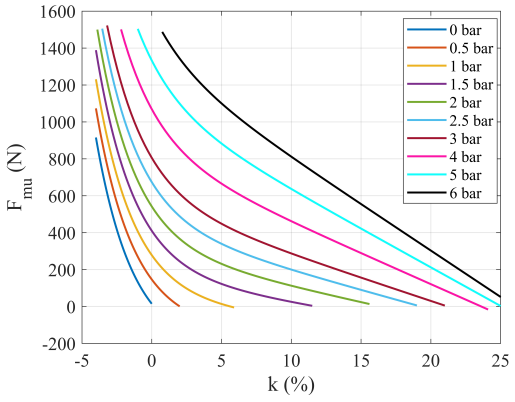

Fig. 3. Static characteristics of the McKibben muscle (DMSP-20-200N, Festo, Germany) at different supply pressures.

When the arm is in its initial position at θ_1=90°, the initial contraction of k_1=5 % is chosen. Therefore, the initial length L_1 is:

$$L_1 = l_0\left(1-\frac{k_1}{100}\right)=0.1995\,m \tag{5}$$

The muscle is pressurized at the desired pressure value, so it contracts lifting the arm until the torque generated by the muscle reaches the static equilibrium with the moment due to gravity. For each elevation angle θ_1 of the arm, the shortening Δb of the wire, which is considered non-extendible, is equal to the contraction of the pneumatic muscle:

$$\Delta b(\theta_1) = b(90^\circ) - b(\theta_1) \tag{6}$$

Finally, the actual length of the pneumatic muscle L and its percentage of contraction k can be calculated:

$$L(\theta_1) = l_0 - \Delta b(\theta_1) \tag{7}$$

$$k(\theta_1) = 100\left(1-\frac{L(\theta_1)}{l_0}\right) \tag{8}$$

By selecting different air pressure p, the tension force F_{mu} can be derived from Eq. (4) for each elevation angle θ_1 and used to estimate the torque M_{mu} exerted by the pneumatic muscle about the shoulder:

$$M_{mu} = F_{mu} r \tag{9}$$

The matching between the device torque M_{mu} and the gravitational load required (Fig. 1) is relevant for the correct functionality of the exoskeleton.

2.2 Cam-based design of the transmission system

With respect to the solution presented in Fig. 2 (left), an additional cam-based architecture has been studied. The adoption of a cam profile for transmitting the force of the actuator to the limb of the operator is aimed at approximating as much as possible the torque generated at the shoulder by the actuator to that created by the gravitational load, so as to extend as much as possible the range of the elevation angle at which the operation is to be performed. The cam profile and position should be selected in order to not disturb the user's view and to avoid increasing the bulkiness of the system with respect to the original design. To this outcome, the cam profile should not exceed the eye position, with respect to the shoulder joint (SJ), that can be estimated from the literature [22].

The proposed architecture is based on a cam profile formed on a rigid shoulder pad centered on the ideal center of the SJ (see Fig. 2, right). The same pneumatic muscle shown in the original design is assumed. The cam design and a scheme of its imple-

mentation in the final device have been performed mainly by graphical approach, as presented in Fig. 4.

In the conceiving of the exoskeleton, it was decided to design it hypothesizing a working range of the elevation angle θ_l between 90° and 135°, assuming assistance for operations in an elevated position. This implies that to move outside this range (particularly in positions below 90°) the operator would have to exert a significant effort at the shoulder level. A non-working position below 90° could be reached by reducing the pressure in the actuator.

For a defined working range of elevation angle and a nominal supply pressure (p=3 bar), the initial lever arm r_i of the muscle force has been deducted from the equilibrium of the gravitational load. To determine the muscle force at θ_l=90°, an initial percentage contraction k_l of 5% has been selected. Then, the desired lever arm r_f of the muscle force at the maximum elevation angle has been chosen, ranging between 40 mm and 70 mm. This range was selected to limit the resulting cam radius, since a large cam profile could be difficult to implement in the final design. The limit values for r_f have been selected by iterative tuning, in order to get force and contraction values that could be achieved by the PAM used, given the static characteristics shown in Fig. 3. The cam profile has been graphically obtained by circular arc interpolation, in particular by ensuring the tangency between the cable and the profile itself, for the initial (θ_l=90°) and final (θ_l=135°) configurations. Intermediate positions were extrapolated from the CAD design and imported into MATLAB to calculate the muscle force lever arm r for each configuration between θ_l=90° and θ_l=135°. Similarly, the free cable length and the resulting percentage contraction k of the PAM were calculated as presented in Eq. (7). Finally, from Eqs. (4) and (9), the muscle tension and torque were respectively evaluated.

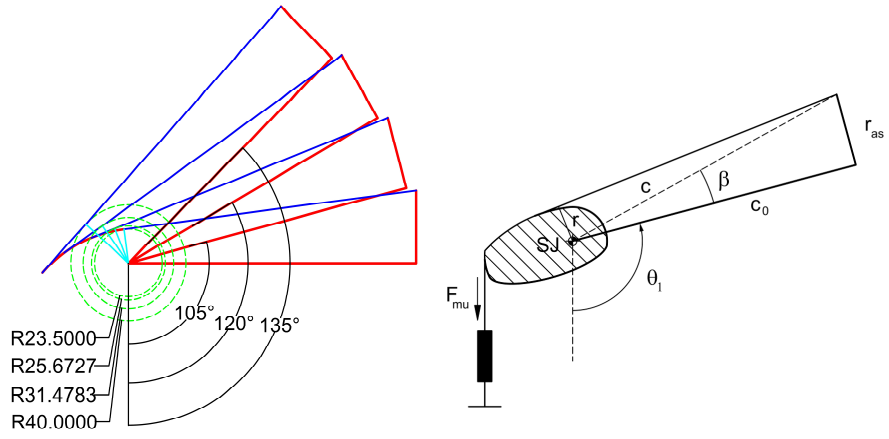

Fig. 4. Cam-based architecture for r_f=40 mm configuration: graphical approach to evaluate cam profile (left), implementation of the cam in the exoskeleton (right).

3 Results and Discussion

The functionality of the exoskeleton depends on the matching between the torque generated by the device and the external load exerted on the arm of the operator. For this reason, the supporting torque provided by the actuator at the SJ was computed for both configurations shown in the previous section and compared to the gravitational load. The configurations tested are briefly resumed in the following:

- Configuration A: original design, cable and pulley transmissions system.
- Configuration B: cam-based transmission system, with the cam centered at the SJ.

The original configuration (A) was tested in a "no load" condition, subjected only to the weight of the arm, and in a loaded condition, with a 1 kg load in the hand. The results of these simulations are presented in Fig. 5.

With respect to Fig. 2 (left), the exoskeleton structure was based on the following geometrical parameters and condition: a=0.15 m, c_0=0.2 m, α=80°, β=14°, θ_2=0°. The loaded condition represents a typical situation in which the user is holding a tool with lifted arms. In this condition, the initial contraction is assumed to be 5% as for the unloaded condition, but it results in a lower equilibrium position as shown in Fig. 5, since the supporting and gravitational torques match at lower elevation angles θ_1. However, even in the "no load" condition, the system could not fulfill one of the most critical specifications of this design, that is an adequate matching between the gravitational torque and the one provided by the device. The difference between the torque profiles shown in Fig. 5 and the torque due to gravity requires an additional contribution from the operator to move the arm within the range of elevation angles selected.

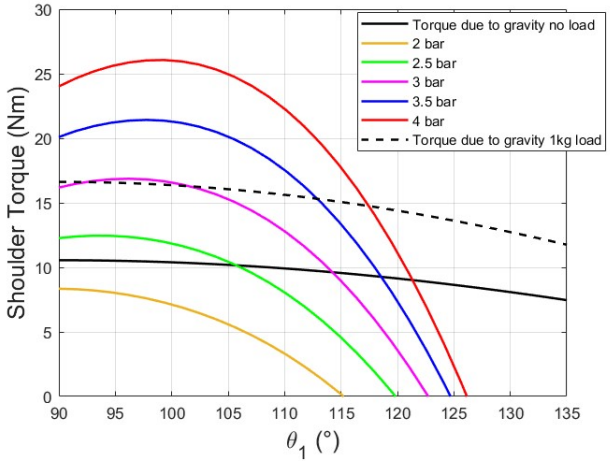

Fig. 5. Torque due to the weight of the arm, in unloaded and loaded condition, and torques exerted by the exoskeleton (configuration A) at different supply pressures.

The performance of the exoskeleton in the original configuration A was then compared to the behavior of the system with the cam-based design (configuration B). The same geometrical parameters used for configuration A were selected (c_0=0.2 m, β=14°, θ_2=0°). Simulations have been made for final lever arm r_f ranging from 40 to 70 mm. The best results have been obtained for r_f equal to 40 and 50 mm and are presented in Fig. 6. The limited mismatch between the torque profiles can be quite easily provided by the user, whose activity can be effectively supported by the device in a very extended working range. Appropriate regulation of the supply pressure can adapt the device action to the operating conditions.

Between the presented solutions, configuration B is the most promising also regarding the reduction of the bulkiness of the system, with the cam, centered at the SJ, being easily integrated within a shoulder pad, without the need for a supporting bar (as the one shown in Fig. 2, on the left, with length a).

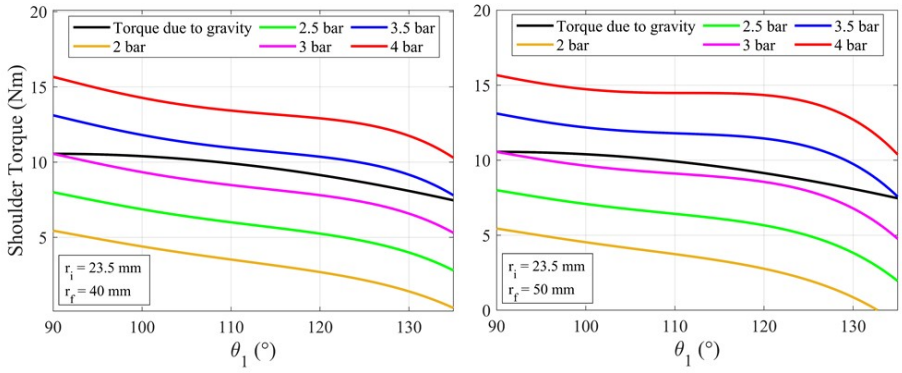

Fig. 6. Torque due to the weight of the arm and torques exerted by the exoskeleton (configuration B) at different supply pressures. Each plot refers to a different value of final lever arm r_f.

4 Conclusion

This study demonstrates the feasibility of a passive exoskeleton for the upper body based on the use of a McKibben pneumatic artificial muscle.

The exoskeleton may effectively support an operator that must perform a task with upper limbs in an elevated position. The performance of the exoskeleton strictly depends on the system of transmission of the actuator force to the operator's limb.

A transmission based on the sliding of a tendon cable on a cam-shaped shoulder strap is particularly convenient, since it allows for extending the compensatory effect of the actuator over an extended working range of the shoulder joint. However, the effectiveness of the result requires an accurate design of the cam profile.

The structure of the exoskeleton may be extremely simple and lightweight. The device may be very easily adapted to the anthropometric characteristic of the operator and to the kind of work that must be performed.

The proposed architecture has been designed to support the upper limb lifted in the sagittal plane. However, limited abduction\adduction and internal\external rotation angles can be allowed by appropriate design of the transmission system, in particular regarding the connection between the bracelet and the fixed frame integral with the trunk. For instance, a 2 DoF joint centered at the SJ could be implemented to allow such movements.

References

1. Gopura, R., Kiguchi, K.: Mechanical designs of active upper-limb exoskeleton robots: State-of-the art and design difficulties. Rehabilitation Robotics ICORR 2009. IEEE International Conference, pp. 178-187 (2009).
2. Sanjuan, J.D., et al.: Cable driven exoskeleton for upper-limb rehabilitation: A design review. Robotics and Autonomous Systems 126, 103445 (2020).
3. Nef, T., et al.: ARMin - Exoskeleton for Arm Therapy in Stroke Patients. 2007 IEEE 10th Inernational Conference on Rehabilitation Robotics, pp. 68-74 (2007).
4. Cappello L., et al.: A series elastic composite actuator for soft arm exosuits. 2015 IEEE International Conference on Rehabilitations Robotics, pp. 61-66 (2015).
5. Perry, J.C., Rosen, J., Burns, S.: Upper-limb powered exoskeleton design. IEEE/ASME Transactions on Mechatronics 12(4), pp. 408-417 (2007).
6. Gopura, R., Kiguchi, K., Yi, Y.: SUEFUL-7: a 7DOF upper-limb exoskeleton robot with muscle-model-oriented EMG-based control. IEEE/RSJ international conference on intelligent robots and systems, pp. 1126-1131 (2009).
7. Lo, H.S., Xie, S.Q.: Exoskeleton robots for upper-limb rehabilitation: State of the art and future prospects. Medical Engineering & Physics 34, pp. 261-268 (2012).
8. Cui, X., et al.: Design of a 7-dof cable driven arm exoskeleton (carex-7) and a controller for dexterous motion training or assistance. IEEE/ASME Trans. Mechatronics 22(1), pp. 161-172 (2017).
9. Park, H.S., Ren, Y., Zhang, L.Q.: IntelliArm: an exoskeleton for diagnosis and treatment of patients with neurological impairments. 2008 2nd IEEE RAS & EMBS International Conference on Biomedical Robotics and Biomechatronics, pp. 109-114 (2008).
10. Dehez, B., Sapin. J.: Shouldero, an alignment-free two-dof rehabilitation robot for the shoulder complex. 2011 IEEE International Conference on Rehabilitations Robotics, pp. 1-8 (2011).
11. He, J., et al.: Rupert: a device for robotic upper extremity repetitive therapy. 2005 IEEE Engineering in Medicine and Biology 27th Annual Conference, pp. 6844-6847 (2005).
12. Sasaki, D., Norisugu, T., Takaiwa M.: Development of active support splint driven by pneumatic soft actuator (ASSIST). Proceedings of the 2005 IEEE International Conference on Robotics and Automation, pp. 520-525 (2005).
13. Klein, J., et al.: Biomimetic orthosis for the neurorehabilitation of the elbow and shoulder (BONES). 2008 2nd IEEE RAS & EMBS International Conference on Biomedical Robotics and Biomechatronics, pp. 535-541 (2008).
14. Tsagarakis, N.G., Caldwell, D.G.: Development and control of a 'Soft-Actuated' exoskeleton for use in physiotherapy and training. Autonomous Robots 15, pp. 21-33 (2003).
15. Rahman, T., et al.: Passive exoskeletons for assisting limb movement. Journal of Rehabilitation Research & Development 43, pp. 583-590 (2006).
16. Rahman, T., et al.: simple technique to passively gravity-balance articulated mechanisms. ASME Trans Mech Des. 117(4), pp. 655–658 (1995).

17. Yin, P., et al.: Effects of a passive upper extremity exoskeleton for overhead tasks. Journal of Electromyography and Kinesiology 55, 102478 (2020).
18. Huysamen, K., et al.: Evaluation of a passive exoskeleton for static upper limb activities. Applied Ergonomics 70, pp. 148-155 (2018).
19. HIEIBER, 2019. Hyetone Industrial EXO Intelligent Boost Exoskeleton Robot (HIEIBER). Guangzhou Hyetone Mechanical and Electrical Equipment Co., Ltd, The China, www.hyetone.com.
20. Maurice, P., et al.: Objective and Subjective Effects of a Passive Exoskeleton in Overhead Work. IEEE Trans Neural Syst Rehabil Eng. 28(1), pp. 152-164 (2019).
21. Zhu, Y., et al.: Automatic load-adapting passive upper limb exoskeleton. Advances in Mechanical Engineering 9, pp. 1-8 (2017).
22. De Leva, P.: Adjustments to Zatsiorsky-Seluyanov's segment inertia parameters. Journal Biomechanics 29(9), pp. 1223-1230 (1996).
23. Pitel, J., Tothova, M.: Modeling of pneumatic muscle actuator using Hill's model with different approximations of static characteristics of artificial muscle. MATEC Web of conferences 76, 02015 (2016).